Earth and Planetary Science Letters 438 (2016) 14–24

Contents lists available at ScienceDirect

Earth and Planetary Science Letters

www.elsevier.com/locate/epsl

Light and variable $^{37}Cl/^{35}Cl$ ratios in rocks from Gale Crater, Mars: Possible signature of perchlorate

K.A. Farley [a,*], P. Martin [a], P.D. Archer Jr. [b], S.K. Atreya [c], P.G. Conrad [d], J.L. Eigenbrode [d], A.G. Fairén [e], H.B. Franz [d,f], C. Freissinet [d], D.P. Glavin [d], P.R. Mahaffy [g], C. Malespin [g], D.W. Ming [b], R. Navarro-Gonzalez [h], B. Sutter [b,i]

[a] Division of Geological and Planetary Sciences, Caltech, Pasadena, CA, USA
[b] Astromaterials Research and Exploration Science Directorate, NASA Johnson Space Center, Houston, TX, USA
[c] Department of Atmospheric, Oceanic, and Space Sciences, University of Michigan, Ann Arbor, MI, USA
[d] Solar System Exploration Division, NASA Goddard Space Flight Center, Greenbelt, MD, USA
[e] Department of Astronomy, Cornell University, Ithaca, NY 14853, USA
[f] Center for Research and Exploration in Space Science and Technology, University of Maryland, Baltimore County, Baltimore, MD, USA
[g] Planetary Environments Laboratory, NASA Goddard Space Flight Center, Greenbelt, MD, USA
[h] Instituto de Ciencias Nucleares, Universidad Nacional Autonoma de Mexico, Ciudad Universitaria, Mexico City, Mexico
[i] Jacobs Technology-ESCG, Houston, TX, USA

ARTICLE INFO

Article history:
Received 8 August 2015
Received in revised form 13 December 2015
Accepted 16 December 2015
Available online 22 January 2016
Editor: T.A. Mather

Keywords:
Mars
Cl isotopes
perchlorate
evolved gas analysis

ABSTRACT

Cl isotope ratios measured on HCl thermally evolved from as-yet-unknown phases in sedimentary rocks and sand in Gale Crater provide unexpected insights to the Martian surficial Cl cycle. The seven samples yield δ^{37}Cl values ranging from -1 ± 25‰ to -51 ± 5‰. Five analyses from two samples of the Sheepbed mudstone (Yellowknife Bay study area) are analytically indistinguishable with a mean δ^{37}Cl of -11 ± 7‰ (1σ). In contrast, four mudstones/sandstones from the Kimberley and Pahrump study areas also yielded indistinguishable ratios, but with a mean δ^{37}Cl of -43 ± 6‰. The Rocknest sand deposit gave a highly uncertain δ^{37}Cl value of -7 ± 44‰.

These light and highly variable δ^{37}Cl values are unique among known solar system materials. Two endmember models are offered to account for these observations, and in both, perchlorate, with its extreme ability to fractionate Cl isotopes, is critical. In the first model, SAM is detecting HCl from an oxychlorine compound (e.g., perchlorate) produced from volcanic gas emissions by atmospheric chemical reactions. Similar reactions in Earth's atmosphere may be responsible for the isotopically lightest known Cl outside of this study, in perchlorate from the Atacama Desert. Some of the Gale Crater δ^{37}Cl values are more negative than those in Atacama perchlorate, but because reaction mechanisms and associated fractionation factors are unknown, it is impossible to assess whether this difference is prohibitive. If the negative δ^{37}Cl signal is produced in this fashion, the isotopic variability among samples could arise either from variations in the relative size of the reactant chloride and product perchlorate reservoirs, or from variations in the fraction of perchlorate reduced back to chloride after deposition. Such reduction strongly enriches ^{37}Cl in the residual perchlorate.

Perchlorate reduction alone offers an alternative endmember model that can explain the observed data if SAM measured HCl derived from chloride. In this model isotopically normal perchlorate produced by an unspecified mechanism is reduced to chloride. Depending on the relative size of the reduced reservoir, the integrated product chloride can vary in isotopic composition from −70‰ in the first increment all the way to the starting composition if the perchlorate is fully reduced. Thus, variable degrees of perchlorate reduction can produce chloride with the appropriate δ^{37}Cl range. Combination of the two endmember models, in which the perchlorate subject to post-deposition reduction is isotopically negative from atmospheric reactions, is also possible.

Determination of the phase hosting the Cl measured by SAM, an oxychlorine compound or chloride, is critical for selecting between these models, and for developing implications of the results for the Mars surficial Cl cycle. At present it is not possible to conclusively establish which phase is responsible

* Corresponding author. Tel.: +1 626 395 6005.
E-mail address: farley@gps.caltech.edu (K.A. Farley).

http://dx.doi.org/10.1016/j.epsl.2015.12.013

(possibly both), but limited evidence favors the conclusion that the measured Cl derives mostly from an oxychlorine compound.

1. Introduction

The Sample Analysis at Mars instrument (Mahaffy et al., 2012) on the Curiosity Rover has measured the volatile composition of ancient sedimentary rocks and a sand drift in Gale Crater (Archer et al., 2014; Glavin et al., 2013; Leshin et al., 2013; McAdam et al., 2014; Ming et al., 2014). HCl is among the most abundant species detected during evolved gas analysis (EGA) of every sample, typically at a level of ~10 μmol/g. Some and possibly all of this chlorine may derive from the decomposition of an oxychlorine species, probably a perchlorate salt (Glavin et al., 2013). The oxychlorine compound accounts for a substantial fraction of the total Cl in these rocks (Archer et al., 2015) and is thought to be an ancient constituent (Ming et al., 2014). Additional HCl could derive from other minerals in the sample (e.g., halite, akaganeite) but such are in low abundance and it is presently unclear whether these minerals can release HCl under the adopted analytical conditions (Glavin et al., 2013). The presence of oxychlorine compounds including perchlorate was recently reported in a martian meteorite (Kounaves et al., 2014).

The isotopic composition of Cl can be measured in the evolved HCl in the SAM quadrupole mass spectrometer (QMS). Although corrections for isobaric species preclude high precision isotope ratio determinations, variability is nevertheless apparent. Here we report unexpectedly light and highly variable $^{37}Cl/^{35}Cl$ ratios, and discuss possible implications. Given our current uncertainty in the mineral host of the Cl, our conclusions are necessarily tentative, but they strongly suggest an important role for oxychlorine compounds, such as perchlorate salts, in Mars surficial Cl cycle.

$^{37}Cl/^{35}Cl$ ratios are reported relative to standard mean ocean chlorine (SMOC, $^{37}Cl/^{35}Cl = 0.31955$, Wei et al., 2012) and using δ notation:

$$\delta^{37}Cl = 1000(R_{sample}/R_{SMOC} - 1); \quad R = {}^{37}Cl/{}^{35}Cl$$

On that scale, most terrestrial materials, including igneous rocks, mantle xenoliths, clastic and evaporitic sediments, seawater, and groundwater chloride vary within just ±3‰ (e.g., Desaulniers et al., 1986; Eggenkamp et al., 1995; Selverstone and Sharp, 2015; Sharp et al., 2007). The only terrestrial material well outside this range is perchlorate salt from the Atacama Desert, with $\delta^{37}Cl$ as low as −15‰ (Bohlke et al., 2005; Jackson et al., 2010). Atacama perchlorate may be produced by atmospheric photochemical reactions followed by dry deposition on to a very arid landscape (Bohlke et al., 2005; Catling et al., 2010). Atmospheric processes are readily apparent in the O-isotope systematics of this perchlorate (Bao and Gu, 2004) and may also account for its uniquely light Cl (Bohlke et al., 2005). Redox reactions are an additional mechanism by which to substantially mass-fractionate Cl. For example, at 25 °C perchlorate $\delta^{37}Cl$ is estimated to be ~ 70‰ heavier than chloride at equilibrium (Schauble et al., 2003) and even heavier at lower temperatures. In contrast, the equilibrium isotopic contrast among a variety of chloride-bearing phases is at most a few ‰ (e.g., Eggenkamp et al., 1995; Luo et al., 2014; Schauble et al., 2003). The overwhelming dominance of chlorides compared with oxidized chlorine compounds (oxychlorines), coupled with these small equilibrium fractionations, likely accounts for the limited terrestrial $\delta^{37}Cl$ range.

$\delta^{37}Cl$ among chondrites varies within the range ±5‰, with the least altered carbonaceous chondrites having SMOC-like values (0.3 ± 0.3‰, Sharp et al., 2013). Based on these data, it has been suggested that the inner solar nebula had a uniform SMOC-like Cl isotope ratio. $\delta^{37}Cl$ values of −1.5 to −3‰ in crystallized brines in chondrite parent bodies indicate only modest mineral–fluid fractionation (Bridges et al., 2004). In contrast to chondrites, lunar $\delta^{37}Cl$ is isotopically heavy (up to +24‰), probably due to the uniquely dry conditions of lunar volcanism causing magmatic Cl to be degassed as a metal chloride rather than HCl (Sharp et al., 2010).

Martian meteorites representing a variety of igneous lithologies vary in $\delta^{37}Cl$ from −3.8 to +1.4‰. This variability is positively correlated with indicators of crustal contamination, leading to the hypothesis that the variability arises from mixing between a light (mantle) reservoir, and isotopically heavy crustal contaminants (Sharp et al., 2011; Shearer et al., 2014). The origin of a primitive mantle component below the presumed SMOC-like solar system value may be related to local nebular processes within the region from which Mars accreted, while the heavy values in the hypothesized crustal contaminant were attributed to the residue of mass-fractionating atmospheric loss of Cl, which then interacted with magmas (Shearer et al., 2014; Williams et al., 2015).

2. Materials and methods

2.1. Samples

Bedrock sedimentary outcrops being investigated by the Curiosity rover represent a sequence of sandstones and mudstones thought to have been deposited shortly after the formation of Gale Crater at ~3.8 Ga (Grotzinger et al., 2015). Sediment, probably derived from the crater rim, was deposited in fluvial, deltaic, and lacustrine environments within a lake partially filling the crater. A few tens to possibly hundreds of meters of such sediments were deposited in a relatively wet climate that persisted for at least 10^5 to 10^6 yrs. At a presently unknown later time the rocks were exhumed, most likely by wind erosion. While the chemical composition of the sedimentary rocks is broadly basaltic, the mineralogical assemblage, including clay minerals and a ubiquitous amorphous component, attests to significant chemical weathering or diagenesis (Bridges et al., 2015; McLennan et al., 2014). Abundant sulfate veins and concretions indicate post-depositional fluid–rock interactions (Nachon et al., 2014; Stack et al., 2014).

We present Cl isotope results for all seven solid samples investigated by Curiosity in the first 1000 sols of the mission, as listed in Table 1. Six of the samples are from sedimentary rocks, and were obtained as cuttings from ~5 cm deep drill holes. The seventh, a sample of windblown sand, was obtained by scooping. The sedimentary rock samples come from three distinct study areas spanning ~70 vertical meters of topography investigated along ~10 km of rover traverse. Two samples of the Sheepbed lacustrine mudstone, called John Klein (JK) and Cumberland (CB), represent the topographically lowest investigated bedrock. Although drilled in the same unit, relative to CB, the JK sample has a higher abundance of diagenetic features including veins and concretions (McLennan et al., 2014). The Windjana sample (WJ) is a thinly bedded cross-bedded sandstone from the Kimberley study area, ~30 m higher than Sheepbed. WJ is notable for its very high abundance of K_2O, potassium feldspar, and magnetite (Treiman et al., 2015). The final three rock samples are finely laminated mudstones drilled in the Pahrump Hills study area (Cavanagh et al., 2015; Gellert et al., 2015; Grotzinger et al., 2015; McLennan et al., 2015).

Table 1
Chlorine isotope data. Samples are listed by study area distinguished by shading. Sample name abbreviations are described in the text; each unique two-letter abbreviation represents a single drilled sample and number suffix indicates replicate analysis number of that sample. Sol refers to the day on the mission when the sample was analyzed. TID is the Sample Analysis at Mars investigation designator for the analysis.

Area	Sample	Sol	TID	Mean[a]		Most Precise Interval			
				δ^{37}Cl (‰)	$\pm\sigma$	Start (s)	Stop (s)	δ^{37}Cl (‰)	$\pm\sigma$
	RN4	117	25 048	−7	44	9612	9792	−36	37
Yellowknife	JK3	224	25 074	−11	10	9684	9864	−12	10
Bay	JK4	227	25 077	−1	25	10 512	10 692	−9	18
	CB2	286	25 091	−14	26	11 108	11 288	−21	23
	CB3	290	25 094	−10	17	11 008	11 188	−11	16
	CB5	382	25 130	−20	4	10 635	10 815	−18	3
	CB-OD2	823	25 231	−16	3	6606	6786	−10	3
Kimberley	WJ	624	25 193	−51	5	8663	8843	−58	3
	WJ-Geo	653	25 202	−49	2				
Pahrump	CH	773	25 226	−37	8	9509	9689	−50	8
	MJ	887	25 242	−41	5	9440	9620	−51	4
	TP	928	25 257	−38	6	8612	8792	−44	6

[a] Average of individual sweep values weighted by uncertainty and Cl abundance.

In ascending stratigraphic order the samples are called Confidence Hills (CH), Mojave (MJ), and Telegraph Peak (TP); these rocks are respectively 58, 59, and 67 m higher than Sheepbed. Diagenetic features are pervasive in the Pahrump Hills section, including sulfate veins and, in the case of MJ, as yet unidentified crystal pseudomorphs. In addition to typical basaltic minerals, rocks of the Pahrump section contain hematite and jarosite (Cavanagh et al., 2015; Leveille et al., 2015).

Cl isotope data are also presented for the Rocknest sample, scooped early in the mission from a modern sand drift deposit (Leshin et al., 2013).

2.2. Methods

Samples were obtained by rotary-percussive drilling or by scooping. After sieving to <150 μm, between 50 and 150 mg portions of sample were introduced into SAM for analysis. The EGA protocol (Archer et al., 2014; Mahaffy et al., 2012) used for most samples is summarized in the supplementary material. For some samples, multiple aliquots of the same drilled material were analyzed, and these are denoted by numerical suffixes appended to the sample abbreviation. Analytical procedures distinct from the standard EGA method were used for two aliquots included in this study. WJ-Geo is an aliquot of the Windjana sandstone analyzed for geochronology using the semi-static protocol (Farley et al., 2014). CB-OD2 is an aliquot of the Cumberland sample analyzed by an EGA technique designed to maximize yield of derivitized organic compounds (Freissinet et al., 2015). As described below these analyses are valuable for establishing repeatability of instrument performance over the course of the mission.

HCl is the most abundant Cl-bearing constituent in the evolved gas mass spectra, typically at the level of 0.1 to 1×10^6 counts per second. For this reason, we used the ratio of signals at masses 38 and 36 to determine the Cl isotope ratio, R_{Cl}. These two masses each have isobaric interferences for which corrections must be made:

$$^{37}Cl/^{35}Cl \equiv R_{Cl} = (H^{37}Cl/H^{35}Cl) = \beta(M_{38} - I_{38})/(M_{36} - I_{36}) \quad (1)$$

where M_x is the signal at mass x and I_x is the sum of signals of the interfering isobars at mass x. The interfering species at mass 36 include $H_2{}^{34}S$, ^{36}Ar, $^{18}O^{18}O$ and the C_3 hydrocarbon fragment. The isobars at mass 38 include the C_3H_2 hydrocarbon fragment and a few minor constituents such as ^{38}Ar, doubly-ionized CS_2, and fragments of acetonitrile (CH_3CN). The β term corrects for experimental and instrumental bias in converting the measured signals to a true isotope ratio in the sample. The supplementary material describes how the isobaric species can be quantified and associated corrections made. The important isobars are the hydrocarbon peaks on both masses and the H_2S isobar on mass 36. The supplementary material also demonstrates how uncertainty in isobaric corrections can be estimated and propagated into the computed Cl isotope ratio.

We use three approaches to characterize the Cl isotopic ratio of our samples. First, we compute the ratio and its uncertainty in each few-second duration sweep of the mass spectrum, yielding a time series over the entire course of the EGA run. Second, we compute an uncertainty-weighted and HCl-weighted mean from the time series data. Third, we compute the Cl isotopic ratio for the specific time interval of the EGA run that minimizes uncertainty in the isotopic ratio. The latter occurs when the isobaric corrections are a minimum. The three methods yield consistent results but provide different ways to view and evaluate the isotope ratios.

For the time series and weighted mean calculations, we computed the uncertainty of the Cl isotope data obtained on each mass spectrometric sweep (see supplementary material). The uncertainty- and chlorine-weighted mean isotope ratio was computed directly from these individual sweep results. Examination of all of our EGA runs demonstrates that the random error associated with the total signal counts becomes a small fraction (<25%) of the total uncertainty (which is then dominated by isobaric correction uncertainties) when data was pooled into 180 s blocks. Therefore running 180 s means were used for plotting the isotope ratio time series. These running mean data were also used to identify the specific 180 s time interval over which the total uncertainty was minimized.

A notable feature of the SAM data is a background signal of HCl increasing over the course of the mission. For example, even before the most recent samples (e.g., Mojave) experienced heating to more than ~100 °C, HCl was detected. This signal likely arises from memory of previous samples released either from the vacuum tubing or surfaces within the QMS. Because the signal intensities are small and isobar corrections are large early in the EGA runs, the Cl isotope ratios are initially highly uncertain but generally SMOC-like. Given this uncertainty and the ambiguity of how this Cl relates to the sample, we focus our analyses on the interval when HCl is clearly being released by most samples. For this purpose we adopted a lower temperature cutoff of 200 °C (150 °C for sample CB5, which has a prominent release starting at this temperature).

Results of this data reduction protocol are illustrated for a typical EGA run (sample WJ) in Fig. 1.

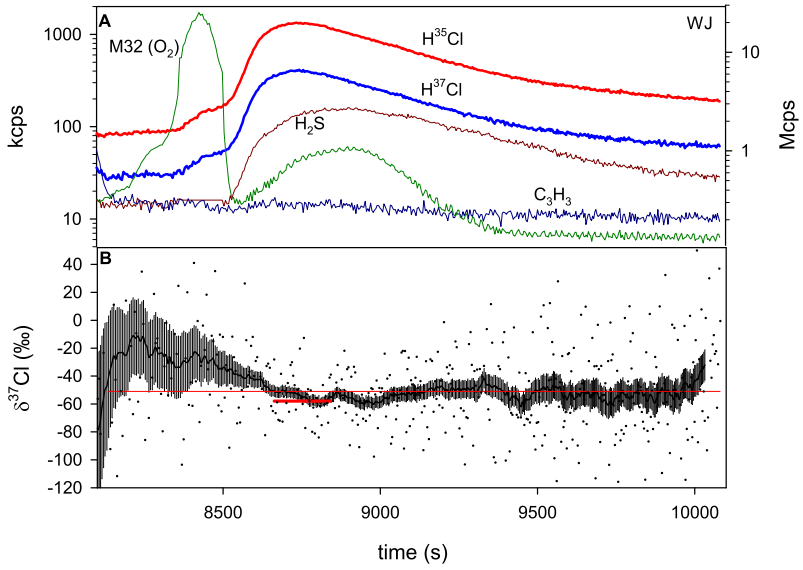

Fig. 1. Typical EGA data, for the Windjana Sample (WJ1). A) deadtime and isobar corrected traces for the two HCl isotopologues and the two peaks used to trace isobaric interferences on them, H_2S and C_3H_3 (all count rates in kcps). Also shown is the evolution of M32, which is dominated by O_2 (count rates in Mcps), signaling the decomposition of an oxychlorine compound. B) Chlorine isotopic composition. The 180 s running mean and associated 1σ uncertainty band is indicated in black. The bold red bar indicates the time interval over which the isotope ratio was most precisely determined (see text), and its associated chlorine isotope ratio. The thin red line is the weighted mean of the evolved chlorine isotope ratio. (For interpretation of the references to color in this figure legend, the reader is referred to the web version of this article.)

The CB-OD2 analysis was very similar to those described above, but with a heating schedule designed to enhance evolved organic molecules. This causes the correction for hydrocarbon contamination on M38 to be larger and therefore more problematic on this run at temperatures <600 °C. To reduce this complication only the high temperature (>600 °C) data were used for isotope ratio determination. The WJ-Geo sample was run in semi-static mode after exposure to getters and a scrubber (Farley et al., 2014). This sample had a very large and stable HCl signal from which to estimate the isotopic ratio. Data for this run were treated similarly to the EGA data in terms of isobar correction. However, in contrast to the EGA runs which record the instantaneous isotopic composition of HCl being swept through the QMS as the sample is heated, the geochronology run integrated all of the gas evolved at ~900 °C. Thus only a single mean ratio is reported and is most properly compared to the weighted mean isotope ratios in the EGA experiments.

Cl isotope measurements were not previously a known application of the SAM instrument, so we have neither Cl isotope standards on board the rover nor pre-flight experiments to constrain instrumental bias. As justified in the supplementary material, to convert from R_{Cl} to δ^{37}Cl we assume that SAM would measure the true ratio (i.e., $\beta = 1$) for standard mean ocean chloride ($^{37}Cl/^{35}Cl = 0.31955$, Wei et al., 2012). We estimate that uncertainty in β adds a systematic uncertainty of perhaps 10‰ to our results. Thus when comparing our results to terrestrial laboratory data this uncertainty in standardization should be recognized; however the relative ratios we report are not affected by this source of uncertainty, and the overarching conclusions not strongly affected.

3. Results

Results are shown as plots against temperature and cumulative chlorine released in Fig. 2 and supplemental Fig. S1. Derived Cl isotope ratios are listed in Table 1.

HCl release from these samples typically begins around ~200 °C, then rises to a prominent maximum around 600–700 °C. In many but not all runs the onset of HCl release coincides with the low temperature O_2 peak attributed to the breakdown of an oxychlorine compound (Ming et al., 2014). Cl isotope ratios at the beginning of the runs are between about 0 and 20‰, usually with large uncertainty owing to the small signal. As the HCl signal rises, the isotope ratio becomes more precise and often declines, becoming invariant as the main HCl peak is swept through. This is readily seen in plots of δ^{37}Cl against cumulative fraction of HCl evolved, where most samples yield stable δ^{37}Cl after the first few to ~15% of the HCl has been released (Figs. 2, S1). Of particular note are the two analyses (CB5, WJ) shown in Fig. 2, because they exhibit very limited variability throughout the entire HCl release. In contrast, sample TP is notable in that a prominent decrease in δ^{37}Cl occurs at about 25% cumulative release. Whether the initial higher ratio is attributable to background HCl in the instrument, or originates in the sample, is difficult to establish. None of the samples have increasing δ^{37}Cl patterns that might suggest progressive distillation of Cl isotopes as the run progresses.

Inspection of both the EGA traces and the isotope ratio evolution plots suggests that each analysis is unique, with variations in total detected HCl, pattern of release against temperature, and isotope ratio evolution. For the purposes of this paper we focus on the most basic aspects of these results, rather than specific interpretations of each run. In particular our main interest is in the bulk-sample Cl isotopic ratios, rather than temporal variations within and among the runs.

Two prominent results from our analyses are that δ^{37}Cl is very negative, as low as −51‰, and highly but systematically variable among samples over the course of the mission (Fig. 3). This conclusion can be drawn equally well from the weighted average Cl isotope ratio and the ratio of the most precisely-measured interval of each sample (Table 1). Analytical uncertainties vary from as low as 2‰ to as high as 44‰, but many results are precise to better than 10‰.

The five EGA-based determinations from the two Sheepbed mudstone samples drilled at Yellowknife Bay (JK3, JK4, CB2, CB3, CB5) yielded analytically consistent δ^{37}Cl values ranging from −1 to −20 and averaging −11‰, with a standard deviation of 7‰. The -16 ± 3‰ ratio for sample CB-OD2 is consistent with these analyses despite its distinctly different analytical protocol. Within the uncertainty level of ~12‰ there is no distinction between JK and CB δ^{37}Cl.

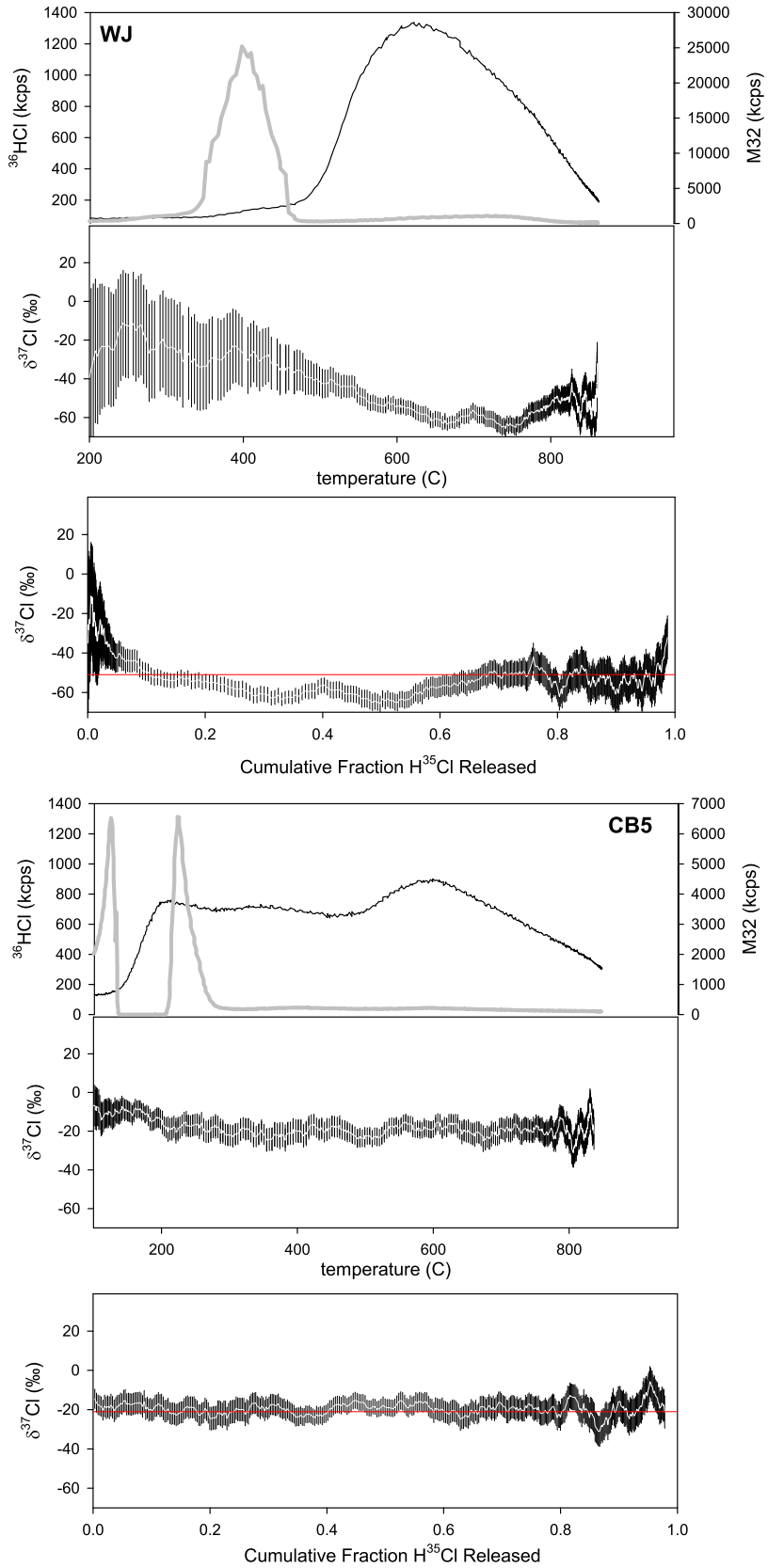

Fig. 2. EGA data as in Fig. 1, but plotted against temperature and the cumulative fraction of HCl released. Results for A) Sample WJ, and B) Sample CB5. The disappearance of the M32 signal at ~200 °C in CB5 is an artifact of detector saturation. These two samples both yield nearly invariant Cl isotope ratios after the onset of HCl release coincident with the major O_2 release.

Samples from Kimberley (WJ) and Pahrump (CH, MJ, TP) yielded more negative δ^{37}Cl, ranging from -37 ± 8‰ to -51 ± 5‰. The average of these values is -43 ± 6‰. The analytically distinct WJ-Geochron run, with a value of -49 ± 2‰, is consistent with

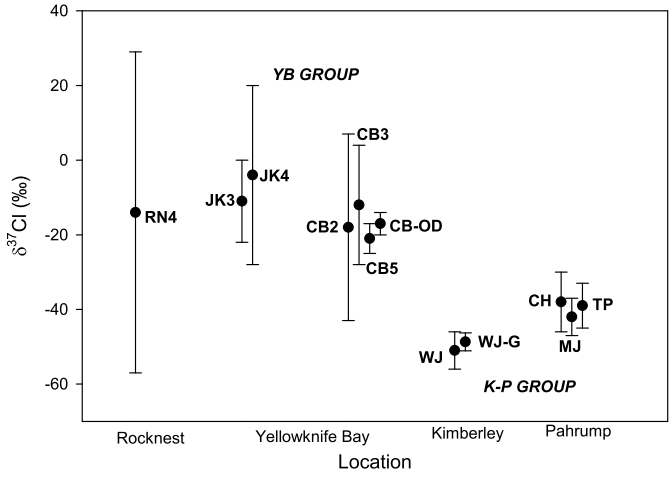

Fig. 3. Chlorine isotope data arrayed as a function of Curiosity's traverse through Gale Crater. Values computed using the most precise time interval are shown. The plot would look nearly identical if the weighted average δ^{37}Cl were plotted instead. The Yellowknife Bay (YB) and Kimberley–Pahrump sample groups are indicated. Designations beside data points are abbreviated sample name and replicate number as described in the text.

other samples from these two regions. The Pahrump region may have isotopic ratios slightly heavier than Kimberley, but not compellingly so given uncertainties.

The Rocknest sand sample (-7 ± 44‰) had an especially low ratio of HCl to hydrocarbons and hence a very large and uncertain isobar correction. No further discussion is given of this sample's highly uncertain δ^{37}Cl.

The ~30‰ difference in δ^{37}Cl between the isotopically consistent samples from Yellowknife Bay and the similarly consistent samples from Kimberley–Pahrump is strikingly large compared to the range previously reported in natural materials. As such it raises the concern of an instrumental artifact, in particular a shift in peak shape or instrument behavior occurring between the Yellowknife Bay and Kimberley campaigns (between sols 382 and 624) that modified the instrumental mass bias. Examination of mass spectra from these and other SAM QMS runs over the same time interval does not support a change in peak shape. More directly, we note that Yellowknife Bay sample CB-OD2 was stored on the rover and analyzed on sol 892, within the time interval of the Kimberley–Pahrump campaigns (sols 624 to 928). Despite this timing, CB-OD2 gives the same ratio as CB and JK samples analyzed in the earlier time interval (sols 224–382). This provides strong evidence against a change in instrumental bias as the source of the observed isotopic contrast.

In the absence of any discernable change in instrument behavior, we conclude that SAM has detected Cl isotopic variability at the ~30‰ level in the sedimentary rocks in Gale Crater. Our best estimate of instrumental bias (essentially none) indicates that these samples are all isotopically light compared to SMOC. At the extreme of our estimate of mass bias uncertainty, the Yellowknife Bay samples may overlap SMOC isotopic composition.

4. Discussion

In this section we seek an explanation for the light and highly variable δ^{37}Cl in our samples. These features are apparent from the entire data set but especially evident in the two key analyses in Fig. 2: CB5 from Yellowknife Bay with a weighted mean δ^{37}Cl of -20 ± 4‰, and WJ from Kimberly at -51 ± 5‰.

4.1. What is the HCl source?

Interpretation of the δ^{37}Cl results requires knowledge of the phase or phases from which Cl was extracted. Unfortunately at present the source phase remains uncertain. At the temperatures involved in the EGA runs, the likely candidates are oxychlorine compounds, chloride salts, and akaganeite (Glavin et al., 2013). Cl in igneous phases (e.g., apatite) is not usually released at these low temperatures (<900 °C). In this section we attempt to constrain which of these phases contributes to the measured HCl signal.

APXS chlorine concentrations in these rocks range from ~0.4 to ~1.4 wt% (Archer et al., 2015; McLennan et al., 2014), but how this element is housed in the rocks is unclear. At Yellowknife Bay and Kimberley, the Chemistry and Mineralogy instrument (Chemin) reported only two minerals with structural Cl: akaganeite and, more speculatively, halite (Vaniman et al., 2014). Oxychlorine compounds were not detected despite the indication of their presence from SAM and APXS data, possibly owing to their low inferred abundance compared to Chemin detection limits, or possibly due to poor crystallinity (e.g., Glavin et al., 2013). The detected phases do not quantitatively account for the APXS Cl concentrations. Taking the Sheepbed rocks as an example, the JK and CB samples have 1.1 and 1.7% akaganeite and ≤0.1% halite, respectively. Even assuming stoichiometric Cl in these phases, and combining them together, they account for <15% of the total Cl detected by APXS. This observation indicates that Cl is either in undetected trace minerals or carried by the X-ray amorphous fraction of these rocks (Dehouck et al., 2014). In the absence of definitive mineralogy, we turn to the EGA traces to help identify likely sources of evolved HCl.

Since HCl is not a constituent of rocks, SAM must be measuring a reaction product between Cl-bearing solid(s) and a hydrogen source. Previous work strongly implicates an oxychlorine compound, possibly a perchlorate salt, as an important source of HCl (e.g., Leshin et al., 2013). This conclusion arises from the release of O_2 at low temperatures and the concordant onset of HCl release (Figs. 1, 2 and Archer et al., 2014; Glavin et al., 2013; Leshin et al., 2013; Ming et al., 2014). The reaction by which an oxychlorine compound decomposes to liberate these gases during EGA heating is complex (Sutter et al., 2015) and since O_2 and HCl are highly reactive, the amount arriving in the mass spectrometer is only a lower limit to the amount in the sample (Ming et al., 2014; Sutter et al., 2015). Comparison of the concentration of O_2 released with the concentration of Cl measured by APXS indicates that the oxychlorine compound accounts for a minimum of between 10 and 40% of the APXS detected Cl in samples JK, CB, WJ, and CH (Archer et al., 2015). The large implied contribution of oxychlorine to total Cl in these rocks is consistent with the results obtained at the Phoenix lander site, in which 5 times more perchlorate was detected than chloride on a molar basis (Hecht et al., 2009).

Laboratory experiments simulating SAM conditions indicate that thermal decomposition of perchlorate salts in various matrices yields a broad HCl peak beginning near the onset of O_2 release and extending to temperatures over 700 °C (Glavin et al., 2013; Sutter et al., 2014, 2015), similar to SAM observations (e.g., Fig. 1). Importantly, although both O_2 and HCl are evolved from perchlorate decomposition, the temporal correlation between O_2 and HCl release in the EGA run is weak. This decoupling must relate to the process by which perchlorate salts decompose and ultimately react to liberate HCl. The temperature of HCl release is sensitive to both the identity of the associated cation and the nature of the matrix in which the perchlorate is heated (Sutter et al., 2014, 2015). SAM EGA traces for HCl, including the release at ~ 600 °C, can be reasonably matched with mixtures of specific perchlorate salts and plausible rock matrices (Glavin et al., 2013;

Sutter et al., 2014, 2015). Taking all of this evidence together, it is likely that a significant portion of the HCl being measured by SAM is derived from one or more oxychlorine compound.

It is less clear whether SAM can detect chloride salts as HCl. While pure anhydrous salts such as halite have too low a vapor pressure (and no H source) to be measured in the temperature range of our experiments, reactions with other species in the sample may promote HCl release. For example, (Glavin et al., 2013) suggested the possibility that at high temperatures (>600 °C), halite in the SAM oven might react with SO_2 to release HCl. This reaction, and possibly others that produce HCl from chloride salts, have not yet been studied under SAM-like conditions. Note that if a substantial fraction of the detected HCl arises from chloride salts, those salts must be too poorly crystalline or too rare to be detected by Chemin in most samples.

Given these considerations, it is not currently possible to conclusively determine whether all of the evolved HCl in our samples derives from an oxychlorine compound, or if instead additional sources, like chloride salts, are also being measured. The rather uniform δ^{37}Cl of some samples, notably CB5 and WJ (Fig. 2), offers an argument in favor of the former for these specific samples, and by extension, the other samples as well. A δ^{37}Cl contrast of up to tens of ‰ is expected between oxychlorine and chloride at equilibrium (Ader et al., 2008; Schauble et al., 2003), and unless chloride and oxychlorine have very similar HCl release patterns with temperature, the absence of significant variation in δ^{37}Cl within these two analyses suggests that just one or the other source is being measured in appreciable abundance. To summarize, an oxychlorine source seems most likely because 1) these samples have a substantial fraction of their Cl accounted for as oxychlorine (Archer et al., 2015), 2) we know SAM can detect oxychlorine compounds, 3) in most samples a rise in the rate of Cl release is coincident with the O_2 release presumed to be from oxychlorine decomposition; and 4) the isotopic composition of most samples is uniform, arguing against multiple sources of isotopically distinct HCl.

4.2. Origin of Cl isotope fractionation

Here we consider processes by which Cl isotope ratios can be fractionated to light values and caused to vary among samples. We start with the assumption that Mars' surficial chlorine originated in the planet's mantle, with δ^{37}Cl within a few ‰ of zero (Williams et al., 2015). Although we prefer the interpretation that we are measuring mainly an oxychlorine compound, we also consider the alternative that we are measuring a chloride. Measurement of both oxychlorine and chloride would imply some mixture of the end-member models described below.

Most natural processes do not strongly fractionate Cl isotopes. For example, the equilibrium fractionation factor between chloride in aqueous solution and single chloride salts like NaCl lies within 0.001 of unity (Eggenkamp et al., 1995; Luo et al., 2014). Taking a fractionation factor of 0.999, even a distilled reservoir in which 99.9% of the chloride has been removed would have δ^{37}Cl shifted by <10‰. The substance we are measuring likely constitutes a substantial fraction of the ~1 weight % of Cl in the samples, so attributing it to the last small increment of distillation is problematic. While a post-fractionation re-concentration process cannot be ruled out, a tiny distilled reservoir is not the most straightforward interpretation. Instead, we focus on mechanisms capable of producing a large reservoir with the requisite isotopic fractionation. There are two leading possibilities: atmospheric escape, and known or hypothesized processes involving oxychlorine chemistry.

4.3. Atmospheric escape

The heavy isotopic composition of many different volatiles attests to extensive mass fractionating loss from the martian atmosphere (Jakosky and Jones, 1997), and Sharp et al. (2011) proposed that some martian meteorites contain Cl fractionated by this process. The possible mechanisms and magnitude of such fractionation have not to our knowledge been modeled. However, the relevant masses of HCl are identical to those of ^{38}Ar/^{36}Ar. SAM recently measured the Mars atmosphere ^{38}Ar/^{36}Ar ratio (Atreya et al., 2013) and confirmed that it is depleted in ^{36}Ar by about 300‰ relative to primordial Ar. This observation suggests that substantial mass fractionation of HCl, presumably emitted from volcanoes into the atmosphere, might be possible. However, unlike Ar, HCl can be removed from the atmosphere by deposition/adsorption on to the surface. This removal would diminish its loss (or the loss of chlorine from HCl photo-dissociation) due to atmospheric escape. More to the point, any mass-fractionating loss of HCl (or any other Cl compound) would leave residual Mars Cl isotopically heavy, rather than light as we observe. Thus atmospheric loss is not a plausible mechanism to explain our observations.

4.4. Oxychlorine chemistry

In this section we consider two different ways in which oxychlorine compounds, especially perchlorate, could yield the Cl isotope ratios we observe at Gale Crater. The two models differ regarding what phase is responsible for the HCl detected by SAM. In Section 4.4.1 we consider an atmospheric process that yields isotopically light oxychlorine. In Section 4.4.2 we consider mass-fractionating oxidation of oxychlorine, which can yield isotopically light chloride.

4.4.1. Atmospheric source of negative δ^{37}Cl – SAM measuring oxychlorine

Of all previously measured materials in the solar system, only natural perchlorate salt from the Atacama Desert has very negative δ^{37}Cl (Bohlke et al., 2005; Jackson et al., 2010). Anomalous Δ^{17}O reveals that at least some of the perchlorate oxygen derives from atmospheric ozone (Bao and Gu, 2004), suggesting that Cl isotope fractionation may also arise in the atmosphere (Bohlke et al., 2005). Atacama perchlorate Cl and O isotopic systematics are distinct from those observed at other locations around the world (Jackson et al., 2010; Poghosyan et al., 2014), indicating that terrestrial perchlorate production involves multiple sources or precursors, and/or multiple perchlorate degradation mechanisms that are not yet understood (Jackson et al., 2010). Indeed, laboratory experiments confirm that perchlorate can be formed from a range of starting materials and environmental conditions, including electrical discharge, ultrasonication, UV and X-ray irradiation, lightning, electron irradiation simulating galactic cosmic ray secondaries, and reactions on aerosols (Carrier and Kounaves, 2015; Dasgupta et al., 2005; Kang et al., 2008; Kim et al., 2013; Kounaves et al., 2014; Rao et al., 2012a, 2012b).

Catling et al. (2010) investigated formation of Atacama perchlorate as a Mars analog, arguing the Atacama environment was most similar to that of Mars. Using a model of atmospheric perchlorate production via gas phase photo-oxidation of volcanic and seasalt derived HCl, these authors obtained a sufficient production rate to account for the perchlorate salt accumulations in the Atacama. However, attempts to extend this model to Amazonian Mars failed to account for the estimated perchlorate inventory in martian surface rocks by orders of magnitude (Smith et al., 2014). More recent work therefore considers other formation pathways, including cosmic ray irradiation of chlorine bearing ices (Kim et al., 2013) and UV irradiation of halite (Carrier and Kounaves, 2015). Because Gale

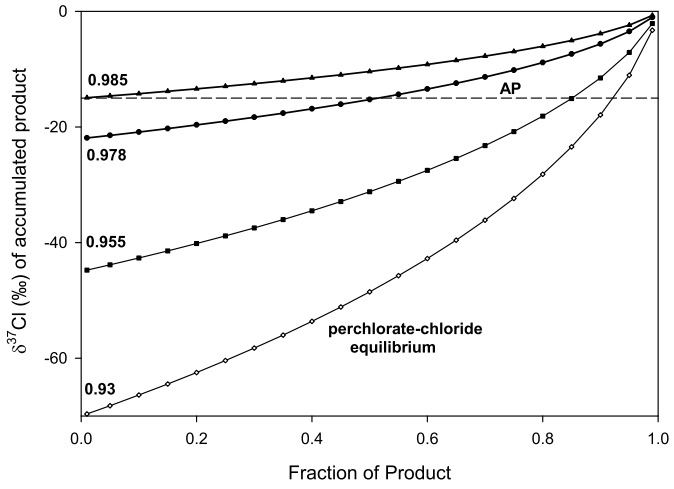

Fig. 4. Rayleigh model for the isotopic composition of an accumulated product plotted for various fractionation factors (labeled) as a function of the fraction of accumulated product for a reactant starting at 0‰. AP denotes the isotopic composition of the most extreme Atacama perchlorate (Bohlke et al., 2005). The maximum fractionation factor that could produce AP is 0.985 and applies to the first increment of perchlorate. Larger extents of reaction of 50% and 80% could yield AP if the fractionation factor were 0.978 or 0.955 respectively. A fractionation factor of 0.955 in atmospheric perchlorate production on Mars could account for the K–P group's δ^{37}Cl of ~ -45‰ starting with a SMOC-like initial atmospheric chloride composition. This same diagram can be used to understand the consequences of perchlorate reduction to chloride and considering the composition of the product chloride. The curve labeled perchlorate–chloride equilibrium traces the isotopic composition of accumulated chloride produced by reduction of perchlorate using the equilibrium fractionation factor (Schauble et al., 2003). This curve suggests that a very wide range of chloride δ^{37}Cl can be produced by partial reduction of perchlorate with normal isotopic composition.

Crater rocks predate the Amazonian and probably formed under very different atmospheric composition, temperature, and density, it is unclear whether any of these models do or do not work to produce the abundance of perchlorate in our samples. For example, models that involve cosmic rays or UV radiation of surface materials may be less effective when the planet's surface is shielded by an atmosphere dense enough to sustain the liquid water evidenced at Gale Crater.

Recognizing the lack of a compelling formation model, we take an empirical approach by comparing our results to Atacama perchlorate simply because this material is the only analog species known to have isotopic characteristics similar to what we observe on Mars. The few Atacama perchlorate samples that have been analyzed have δ^{37}Cl ranging from about -10 to -15‰ (Bohlke et al., 2005; Jackson et al., 2010). Because chemical reactions that reduce perchlorate strongly fractionate it towards heavier δ^{37}Cl (Ader et al., 2008; Sturchio et al., 2007) the most negative reported value is the heaviest possible ratio for the accumulated atmospheric product. Assuming the source of Cl in atmospheric production is isotopically normal (near SMOC; e.g., volcanic or seasalt origin, Catling et al., 2010) and that -15‰ represents the isotopic composition of the first small increment of perchlorate production, the implied fractionation factor for chloride $\rightarrow$ perchlorate in the terrestrial atmosphere is $\alpha_{c\text{-}p} = 0.985$. This is shown graphically in Fig. 4, which plots the isotopic composition of the accumulated distillate of a Rayleigh process as a function of the fraction of product and the fractionation factor. This figure shows that if the Atacama perchlorate is the accumulated distillate of a reaction with a starting reactant composition of $\delta^{37}\text{Cl} = 0$, then the fractionation factor must be $\leq$0.985. For example, if 50% of the available chloride is oxidized to perchlorate, then $\alpha_{c\text{-}p} = 0.978$, and for 85%, $\alpha_{c\text{-}p} = 0.955$. We are not aware of estimates or models that constrain specific values for the fraction of chloride oxidized and/or the associated fractionation factor during possible atmospheric perchlorate production. Because the lowest δ^{37}Cl ratio on Mars (~ -43‰, the mean of the K–P group) is lower than in Atacama perchlorate, so too must the fractionation factor be lower. As shown in Fig. 4, if this mechanism applies and solely accounts for the observed isotopic composition of -43‰, it must have a fractionation factor $<$0.955. Thus this mechanism could be disproven if found to be inadequately fractionating.

In this first endmember model the partial oxidation of volcanic chlorine in Mars' atmosphere yields an isotopically light perchlorate reservoir and a complementary heavy chloride reservoir. We envision that the perchlorate and chloride are both deposited on the martian surface, where they are transported as very soluble anions in surface or groundwater. Like chloride, as the solution evaporates or freezes, perchlorate will precipitate as a salt of a cation governed by the bulk chemistry of the brine. For example, at the Phoenix site the likely salts are K, Mg, and Na perchlorate (Marion et al., 2010). We lack the necessary data to make similar predictions for possible perchlorate salts in Gale Crater rocks. Although some Cl isotopic fractionation is likely between various salts as they precipitate, because no oxidation state change is involved the effect is likely to be modest compared to the magnitude of variability we observe. These salts (or at least the perchlorate) were then trapped in the rock, presumably during or shortly after deposition (Ming et al., 2014) probably in the late Hesperian.

This scenario leads in a straightforward way to the detection by SAM of isotopically light Cl, directly from the decomposition of perchlorate in the SAM oven. The δ^{37}Cl variability among samples could then arise from at least two potential sources: variations in the fraction of the atmospheric Cl reservoir oxidized (e.g., Fig. 4), and mass fractionation associated with post-deposition perchlorate reduction through intermediate oxychlorine compounds ultimately back to chloride.

The maximum fractionation for an accumulated product occurs for the smallest fraction converted, while complete conversion yields no fractionation (Fig. 4). Thus one possible explanation for the observed δ^{37}Cl contrast is that the fraction of chloride oxidized to perchlorate in the atmosphere varied, with greater oxidation recorded by the YB group compared to the K–P group. As an example, if we assume a fractionation factor of 0.955 during atmospheric perchlorate production, then the δ^{37}Cl of the K–P group could be accounted for by a few percent of oxidation, yielding an accumulated perchlorate reservoir of ~ -45‰. In contrast, if the YB group accumulated perchlorate from 80% oxidation of the initial source chloride reservoir, the resulting perchlorate would have δ^{37}Cl of -20‰, close to the observed value. Such an explanation predicts that periods of greater perchlorate production (and higher perchlorate/Cl deposition ratio) would produce perchlorate with higher δ^{37}Cl. However, because the chlorine in these rocks has almost certainly been redistributed and possibly chemically fractionated by dissolution and precipitation in ground and surface waters, it is unclear whether this evidence would be retained in any single rock.

In their modeling study of the Mars atmosphere, Smith et al. (2014) found that perchlorate production is enhanced by more oxidizing conditions. Thus because the atmosphere of early Mars may have been more reducing than present, perchlorate production may have been less efficient and more mass-fractionating earlier in Mars' history. If Mars evolved along a monotonic path from reducing to oxidizing conditions, this hypothesis and the relative δ^{37}Cl we observe could imply that the YB group is younger than the K–P Group. While the stratigraphic relationship between the two sample sets is not entirely clear, Yellowknife Bay may be structurally deepest and hence may comprise the oldest material yet investigated by Curiosity (Grotzinger et al., 2015). If so, this prediction is not supported.

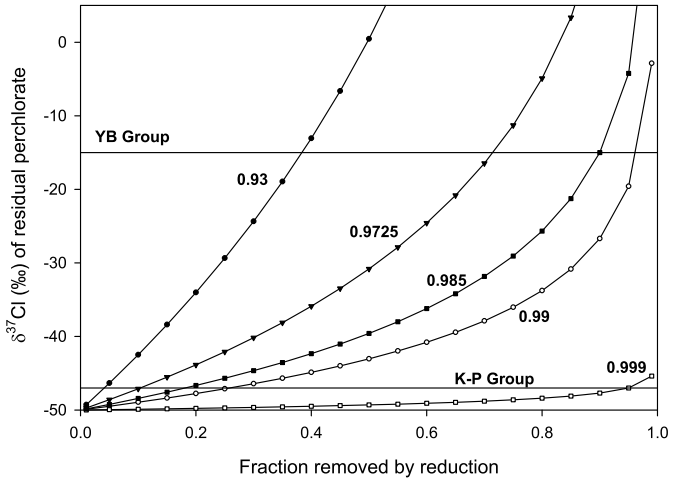

Fig. 5. Model Rayleigh distillation curve showing the isotopic composition of a residual reactant reservoir as a function of the fraction of reactant consumed, for various fractionation factors (indicated). YB and K–P groups indicate δ^{37}Cl composition of the two sample groups. These curves show that fractionation factors of ~0.999 produce very modest isotopic effects. Starting with perchlorate with K–P composition, these curves reveal the combination of fractionation factor and extent of reaction required to yield the YB composition. For example, using the perchlorate–chloride fractionation factor of ~0.93 (Schauble et al., 2003), only about 30% of the perchlorate needs to be reduced to move from the K–P group to the YB group composition.

Alternatively, the δ^{37}Cl variability we observe may reflect processes occurring after arrival of isotopically light perchlorate on the Martian surface, either during aqueous processing and transport, or after deposition of the rock. Reduction of perchlorate to chloride can induce large increases in δ^{37}Cl in residual perchlorate for modest extents of reduction. As shown in Fig. 5, the observed 30‰ shift in δ^{37}Cl of perchlorate would be expected for reduction of just 35% of the perchlorate to chloride using the modeled equilibrium fractionation factor of ~0.93 (Schauble et al., 2003). A similar degree of enrichment could be achieved with other oxychlorine compounds (with fraction factors somewhat closer to unity, Schauble et al., 2003) by allowing a greater extent of reduction. Mechanisms for oxychlorine reduction, including via exposure to ionizing radiation, have been discussed (Quinn et al., 2013). An important unresolved question is whether such reactions would proceed at isotopic equilibrium; in this regard we note that biological reduction of perchlorate to chloride is less mass fractionating than the equilibrium fractionation factor implies (Ader et al., 2008).

4.4.2. Perchlorate reduction source of negative δ^{37}Cl – measuring chloride

The partial reduction of perchlorate described in the previous section offers an alternative endmember model for creating the observed δ^{37}Cl compositions, provided SAM is measuring the composition of a chloride salt rather than an oxychlorine compound. With a fractionation factor of ~0.93 (Schauble et al., 2003), partial reduction of isotopically normal perchlorate can produce extremely negative δ^{37}Cl in chloride (Fig. 4). Again considering the accumulated product of Rayleigh distillation, equilibrium reduction of ~50% of perchlorate to chloride would yield chloride with δ^{37}Cl of −50‰, similar to the K–P samples. To achieve the −20‰ δ^{37}Cl values seen in the YB group samples would require 90% reduction of the starting perchlorate. Variations on this model, involving less oxidized oxychlorine samples, or a perchlorate source that starts out isotopically light, are also possible and would require different extents of perchlorate reduction.

A potential complicating factor with this model is the requirement to keep the perchlorate-derived chloride reservoir separate from extensive dilution with isotopically more-normal sources of chloride. If less than ~50% of the chloride derives from isotopically normal perchlorate, the most extreme observed δ^{37}Cl cannot be obtained by this mechanism. Viewed differently, mixing of perchlorate-derived chloride with isotopically normal chloride (e.g., from weathering of igneous rocks or direct volcanic fallout) offers an additional source of δ^{37}Cl variability if SAM is detecting HCl dominantly from a chloride salt.

5. Conclusions

Sedimentary rocks analyzed by SAM in Gale Crater have very light and highly variable δ^{37}Cl values that provide insights to its mineralogical host and the behavior of Cl on the surface of Mars. Two endmember models that may account for the extremely negative values hinge on the unusual properties of perchlorate. If SAM is measuring the isotopic composition of Cl evolved directly from oxychlorine compounds, then the source of the light Cl may be atmospheric chemical reactions. This possibility is supported by analogy to low δ^{37}Cl perchlorate salts in the Atacama Desert (Bohlke et al., 2005). Alternatively, if SAM is measuring Cl evolved from chloride, partial reduction of isotopically normal perchlorate from an unspecified mechanism is capable of fractionating product chloride to the observed δ^{37}Cl values. For both models the observed isotopic variability may arise from varying extents of highly mass-fractionating oxychlorine reduction among the analyzed samples. Selection between these models requires further work to establish under what conditions SAM can detect HCl from oxychlorine and from chloride salts. Ideally it will be possible to rule out a source based on either the efficiency of the detection, or the temperature of HCl release compared to observations on Mars.

Both hypothetical origins for the low δ^{37}Cl values in Gale Crater rocks offer an alternative explanation to atmospheric escape for the heavy Cl observed in martian meteorites thought to be affected by crustal contamination (Shearer et al., 2014). In particular, these rocks may have experienced assimilation of a component carrying Cl that is the isotopic complement to that detected by SAM. Direct measurement of the Cl-isotopic composition of oxychlorines recently discovered in a martian meteorite (Kounaves et al., 2014) would have direct bearing on this question. A better understanding of perchlorate production, especially under conditions pertaining during the late Hesperian, would be valuable in interpreting our results and in better understanding the martian surficial Cl cycle and its variations through time.

Acknowledgements

This work was supported by the National Aeronautics and Space Administration. This work benefited from several anonymous reviews.

Appendix A. Supplementary material

Supplementary material related to this article can be found online at http://dx.doi.org/10.1016/j.epsl.2015.12.013.

References

Ader, M., Chaudhuri, S., Coates, J.D., Coleman, M., 2008. Microbial perchlorate reduction: a precise laboratory determination of the chlorine isotope fractionation and its possible biochemical basis. Earth Planet. Sci. Lett. 269, 604–612.

Archer, P.D., Franz, H.B., Sutter, B., Arevalo, R.D., Coll, P., Eigenbrode, J.L., Glavin, D.P., Jones, J.J., Leshin, L.A., Mahaffy, P.R., McAdam, A.C., McKay, C.P., Ming, D.W., Morris, R.V., Navarro-Gonzalez, R., Niles, P.B., Pavlov, A., Squyres, S.W., Stern, J.C., Steele, A., Wray, J.J., 2014. Abundances and implications of volatile-bearing species from evolved gas analysis of the Rocknest aeolian deposit, Gale Crater, Mars. J. Geophys. Res., Planets 119, 237–254.

Archer, P.D., Ming, D.W., Sutter, B., Morris, R.V., Clark, B.C., Mahaffy, P.H., Wray, J.J., Fairen, A.G., Gellert, R., Yen, A.S., Blake, D.F., Vaniman, D.T., Glavin, D.T., Eigenbrode, J.L., Trainer, M.G., Navarro-Gonzalez, R., McKay, C.P., Freissinet, C., 2015.

Oxychlorine species on Mars: the Gale Crater story. In: 46th Lunar and Planetary Science Conference, p. 2971.
Atreya, S.K., Trainer, M.G., Franz, H.B., Wong, M.H., Manning, H.L.K., Malespin, C.A., Mahaffy, P.R., Conrad, P.G., Brunner, A.E., Leshin, L.A., Jones, J.H., Webster, C.R., Owen, T.C., Pepin, R.O., Navarro-Gonzalez, R., 2013. Primordial argon isotope fractionation in the atmosphere of Mars measured by the SAM instrument on Curiosity and implications for atmospheric loss. Geophys. Res. Lett. 40, 5605–5609.
Bao, H.M., Gu, B.H., 2004. Natural perchlorate has a unique oxygen isotope signature. Environ. Sci. Technol. 38, 5073–5077.
Bohlke, J.K., Sturchio, N.C., Gu, B.H., Horita, J., Brown, G.M., Jackson, W.A., Batista, J., Hatzinger, P.B., 2005. Perchlorate isotope forensics. Anal. Chem. 77, 7838–7842.
Bridges, J.C., Banks, D.A., Smith, M., Grady, M.M., 2004. Halite and stable chlorine isotopes in the Zag H3-6 breccia. Meteorit. Planet. Sci. 39, 657–666.
Bridges, J.C., Schwenzer, S.P., Leveille, R., Westall, F., Wiens, R.C., Mangold, N., Bristow, T., Edwards, P., Berger, G., 2015. Diagenesis and clay mineral formation at Gale Crater, Mars. J. Geophys. Res., Planets 120, 1–19.
Carrier, B.L., Kounaves, S.P., 2015. The origins of perchlorate in the Martian soil. Geophys. Res. Lett. 42, 3739–3745.
Catling, D.C., Claire, M.W., Zahnle, K.J., Quinn, R.C., Clark, B.C., Hecht, M.H., Kounaves, S., 2010. Atmospheric origins of perchlorate on Mars and in the Atacama. J. Geophys. Res., Planets 115, 15.
Cavanagh, P.D., Bish, D., Blake, D., Vaniman, D., Morris, R.V., Ming, D., Rampe, E.B., Achilles, C.N., Chipera, S.J., Treiman, A., Downs, R.T., Morrrison, S.M., Fendrich, K.V., Yen, A.S., Grotzinger, J., Crisp, J., Bristow, T., Sarrazin, P., Farmer, J., Des Marais, D., Stolper, E.M., Morookian, J.M., Wilson, M.A., Spanovich, N., Anderson, R.C., 2015. Confidence Hills mineralogy and CHEMIN results from base of Mt. Sharp, Pahrump Hills, Gale Crater, Mars. In: 46th Lunar and Planetary Science Conference, p. 2735.
Dasgupta, P.K., Martinelango, P.K., Jackson, W.A., Anderson, T.A., Tian, K., Tock, R.W., Rajagopalan, S., 2005. The origin of naturally occurring perchlorate: the role of atmospheric processes. Environ. Sci. Technol. 39, 1569–1575.
Dehouck, E., McLennan, S.M., Meslin, P.Y., Cousin, A., 2014. Constraints on abundance, composition, and nature of X-ray amorphous components of soils and rocks at Gale crater, Mars. J. Geophys. Res., Planets 119, 2640–2657.
Desaulniers, D.E., Kaufmann, R.S., Cherry, J.A., Bentley, H.W., 1986. ^{37}Cl–^{35}Cl variations in a diffusion-controlled groundwater system. Geochim. Cosmochim. Acta 50, 1757–1764.
Eggenkamp, H.G.M., Kreulen, R., van Groos, A.F.K., 1995. Chlorine stable isotope fractionation in evaporites. Geochim. Cosmochim. Acta 59, 5169–5175.
Farley, K.A., Malespin, C., Mahaffy, P., Grotzinger, J.P., Vasconcelos, P.M., Milliken, R.E., Malin, M., Edgett, K.S., Pavlov, A.A., Hurowitz, J.A., Grant, J.A., Miller, H.B., Arvidson, R., Beegle, L., Calef, F., Conrad, P.G., Dietrich, W.E., Eigenbrode, J., Gellert, R., Gupta, S., Hamilton, V., Hassler, D.M., Lewis, K.W., McLennan, S.M., Ming, D., Navarro-Gonzalez, R., Schwenzer, S.P., Steele, A., Stolper, E.M., Sumner, D.Y., Vaniman, D., Vasavada, A., Williford, K., Wimmer-Schweingruber, R.F., MSL Science Team, 2014. In situ radiometric and exposure age dating of the Martian surface. Science 343.
Freissinet, C., Glavin, D., Buch, A., Szopa, C., Kashyap, S., Franz, H., Eigenbrode, J., Brinckerhoff, W.B., Navarro-Gonzalez, R., Teinturier, S., Malespin, C., Prats, B., Mahaffy, P., 2015. First in situ wet chemistry experiment on Mars using the SAM instrument: MTBSTFA derivatization on a martian mudstone. In: 46th Lunar and Planetary Science Conference, p. 2934.
Gellert, R., Berger, J.A., Boyd, N., Campbell, J.L., Desouza, E.D., Elliott, B., Fisk, M., Pavri, B., Perrett, G.M., Schmidt, M., Thompson, L., VanBommel, S., Yen, A.S., 2015. Chemical evidence for an aqueous history at Pahrump, Gale Crater, Mars, as seen by the APXS. In: 46th Lunar and Planetary Science Conference, p. 1855.
Glavin, D.P., Freissinet, C., Miller, K.E., Eigenbrode, J.L., Brunner, A.E., Buch, A., Sutter, B., Archer, P.D., Atreya, S.K., Brinckerhoff, W.B., Cabane, M., Coll, P., Conrad, P.G., Coscia, D., Dworkin, J.P., Franz, H.B., Grotzinger, J.P., Leshin, L.A., Martin, M.G., McKay, C., Ming, D.W., Navarro-Gonzalez, R., Pavlov, A., Steele, A., Summons, R.E., Szopa, C., Teinturier, S., Mahaffy, P.R., 2013. Evidence for perchlorates and the origin of chlorinated hydrocarbons detected by SAM at the Rocknest aeolian deposit in Gale Crater. J. Geophys. Res., Planets 118, 1955–1973.
Grotzinger, J.P., Gupta, S., Malin, M.C., Rubin, D.M., Schieber, J., Siebach, K., Sumner, D.Y., Stack, K.M., Vasavada, A.R., Arvidson, R.E., Calef 3rd, F., Edgar, L., Fischer, W.F., Grant, J.A., Griffes, J., Kah, L.C., Lamb, M.P., Lewis, K.W., Mangold, N., Minitti, M.E., Palucis, M., Rice, M., Williams, R.M.E., Yingst, R.A., Blake, D., Blaney, D., Conrad, P., Crisp, J., Dietrich, W.E., Dromart, G., Edgett, K.S., Ewing, R.C., Gellert, R., Hurowitz, J.A., Kocurek, G., Mahaffy, P., McBride, M.J., McLennan, S.M., Mischna, M., Ming, D., Milliken, R., Newsom, H., Oehler, D., Parker, T.J., Vaniman, D., Wiens, R.C., Wilson, S.A., 2015. Deposition, exhumation, and paleoclimate of an ancient lake deposit, Gale Crater, Mars. Science 350, aac7575.
Hecht, M.H., Kounaves, S.P., Quinn, R.C., West, S.J., Young, S.M.M., Ming, D.W., Catling, D.C., Clark, B.C., Boynton, W.V., Hoffman, J., DeFlores, L.P., Gospodinova, K., Kapit, J., Smith, P.H., 2009. Detection of perchlorate and the soluble chemistry of martian soil at the phoenix lander site. Science 325, 64–67.
Jackson, W.A., Bohlke, J.K., Gu, B.H., Hatzinger, P.B., Sturchio, N.C., 2010. Isotopic composition and origin of indigenous natural perchlorate and co-occurring nitrate in the southwestern United States. Environ. Sci. Technol. 44, 4869–4876.
Jakosky, B.M., Jones, J.H., 1997. The history of Martian volatiles. Rev. Geophys. 35, 1–16.
Kang, N., Jackson, W.A., Dasgupta, P.K., Anderson, T.A., 2008. Perchlorate production by ozone oxidation of chloride in aqueous and dry systems. Sci. Total Environ. 405, 301–309.
Kim, Y.S., Wo, K.P., Maity, S., Atreya, S.K., Kaiser, R.I., 2013. Radiation-induced formation of chlorine oxides and their potential role in the origin of martian perchlorates. J. Am. Chem. Soc. 135, 4910–4913.
Kounaves, S.P., Carrier, B.L., O'Neil, G.D., Stroble, S.T., Claire, M.W., 2014. Evidence of martian perchlorate, chlorate, and nitrate in Mars meteorite EETA79001: implications for oxidants and organics. Icarus 229, 206–213.
Leshin, L.A., Mahaffy, P.R., Webster, C.R., Cabane, M., Coll, P., Conrad, P.G., Archer, P.D., Atreya, S.K., Brunner, A.E., Buch, A., Eigenbrode, J.L., Flesch, G.J., Franz, H.B., Freissinet, C., Glavin, D.P., McAdam, A.C., Miller, K.E., Ming, D.W., Morris, R.V., Navarro-Gonzalez, R., Niles, P.B., Owen, T., Pepin, R.O., Squyres, S., Steele, A., Stern, J.C., Summons, R.E., Sumner, D.Y., Sutter, B., Szopa, C., Teinturier, S., Trainer, M.G., Wray, J.J., Grotzinger, J.P., MSL Science Team, 2013. Volatile, isotope, and organic analysis of Martian fines with the Mars curiosity rover. Science 341.
Leveille, R., Oehler, D., Fairen, A.G., Clark, B., Niles, P.B., Blank, J.G., 2015. Jarosite in Gale Crater, Mars: the importance of temporal and spatial variability and implications for habitability. In: Astrobiology Conference 2015, p. 7307.
Luo, C.G., Xiao, Y.K., Wen, H.J., Ma, H.Z., Ma, Y.Q., Zhang, Y.L., Zhang, Y.X., He, M.Y., 2014. Stable isotope fractionation of chlorine during the precipitation of single chloride minerals. Appl. Geochem. 47, 141–149.
Mahaffy, P.R., Webster, C.R., Cabane, M., Conrad, P.G., Coll, P., Atreya, S.K., Arvey, R., Barciniak, M., Benna, M., Bleacher, L., Brinckerhoff, W.B., Eigenbrode, J.L., Carignan, D., Cascia, M., Chalmers, R.A., Dworkin, J.P., Errigo, T., Everson, P., Franz, H., Farley, R., Feng, S., Frazier, G., Freissinet, C., Glavin, D.P., Harpold, D.N., Hawk, D., Holmes, V., Johnson, C.S., Jones, A., Jordan, P., Kellogg, J., Lewis, J., Lyness, E., Malespin, C.A., Martin, D.K., Maurer, J., McAdam, A.C., McLennan, D., Nolan, T.J., Noriega, M., Pavlov, A.A., Prats, B., Raaen, E., Sheinman, O., Sheppard, D., Smith, J., Stern, J.C., Tan, F., Trainer, M., Ming, D.W., Morris, R.V., Jones, J., Gundersen, C., Steele, A., Wray, J., Botta, O., Leshin, L.A., Owen, T., Battel, S., Jakosky, B.M., Manning, H., Squyres, S., Navarro-Gonzalez, R., McKay, C.P., Raulin, F., Sternberg, R., Buch, A., Sorensen, P., Kline-Schoder, R., Coscia, D., Szopa, C., Teinturier, S., Baffes, C., Feldman, J., Flesch, G., Forouhar, S., Garcia, R., Keymeulen, D., Woodward, S., Block, B.P., Arnett, K., Miller, R., Edmonson, C., Gorevan, S., Mumm, E., 2012. The sample analysis at Mars investigation and instrument suite. Space Sci. Rev. 170, 401–478.
Marion, G.M., Catling, D.C., Zahnle, K.J., Claire, M.W., 2010. Modeling aqueous perchlorate chemistries with applications to Mars. Icarus 207, 675–685.
McAdam, A.C., Franz, H.B., Sutter, B., Archer, P.D., Freissinet, C., Eigenbrode, J.L., Ming, D.W., Atreya, S.K., Bish, D.L., Blake, D.F., Bower, H.E., Brunner, A., Buch, A., Glavin, D.P., Grotzinger, J.P., Mahaffy, P.R., McLennan, S.M., Morris, R.V., Navarro-Gonzalez, R., Rampe, E.B., Squyres, S.W., Steele, A., Stern, J.C., Sumner, D.Y., Wray, J.J., 2014. Sulfur-bearing phases detected by evolved gas analysis of the Rocknest aeolian deposit, Gale Crater, Mars. J. Geophys. Res., Planets 119, 373–393.
McLennan, D., Dehouck, E., Grotzinger, J., Hurowitz, J., Mangold, N., Siebach, K., 2015. Geochemical record of open-system chemical weathering at gale crater and implications for paleoclimates on Mars. In: 46th Lunar and Planetary Science Conference, p. 2533.
McLennan, S.M., Anderson, R.B., Bell, J.F., Bridges, J.C., Calef, F., Campbell, J.L., Clark, B.C., Clegg, S., Conrad, P., Cousin, A., Des Marais, D.J., Dromart, G., Dyar, M.D., Edgar, L.A., Ehlmann, B.L., Fabre, C., Forni, O., Gasnault, O., Gellert, R., Gordon, S., Grant, J.A., Grotzinger, J.P., Gupta, S., Herkenhoff, K.E., Hurowitz, J.A., King, P.L., Le Mouelic, S., Leshin, L.A., Leveille, R., Lewis, K.W., Mangold, N., Maurice, S., Ming, D.W., Morris, R.V., Nachon, M., Newsom, H.E., Ollila, A.M., Perrett, G.M., Rice, M.S., Schmidt, M.E., Schwenzer, S.P., Stack, K., Stolper, E.M., Sumner, D.Y., Treiman, A.H., VanBommel, S., Vaniman, D.T., Vasavada, A., Wiens, R.C., Yingst, R.A., MSL Science Team, 2014. Elemental geochemistry of sedimentary rocks at Yellowknife Bay, Gale Crater, Mars. Science 343.
Ming, D.W., Archer, P.D., Glavin, D.P., Eigenbrode, J.L., Franz, H.B., Sutter, B., Brunner, A.E., Stern, J.C., Freissinet, C., McAdam, A.C., Mahaffy, P.R., Cabane, M., Coll, P., Campbell, J.L., Atreya, S.K., Niles, P.B., Bell, J.F., Bish, D.L., Brinckerhoff, W.B., Buch, A., Conrad, P.G., Des Marais, D.J., Ehlmann, B.L., Fairen, A.G., Farley, K., Flesch, G.J., Francois, P., Gellert, R., Grant, J.A., Grotzinger, J.P., Gupta, S., Herkenhoff, K.E., Hurowitz, J.A., Leshin, L.A., Lewis, K.W., McLennan, S.M., Miller, K.E., Moersch, J., Morris, R.V., Navarro-Gonzalez, R., Pavlov, A.A., Perrett, G.M., Pradler, I., Squyres, S.W., Summons, R.E., Steele, A., Stolper, E.M., Sumner, D.Y., Szopa, C., Teinturier, S., Trainer, M.G., Treiman, A.H., Vaniman, D.T., Vasavada, A.R., Webster, C.R., Wray, J.J., Yingst, R.A., MSL Science Team, 2014. Volatile and organic compositions of sedimentary rocks in Yellowknife Bay, Gale Crater, Mars. Science 343.
Nachon, M., Clegg, S.M., Mangold, N., Schroder, S., Kah, L.C., Dromart, G., Ollila, A., Johnson, J.R., Oehler, D.Z., Bridges, J.C., Le Mouelic, S., Forni, O., Wiens, R.C., Anderson, R.B., Blaney, D.L., Bell, J.F., Clark, B., Cousin, A., Dyar, M.D., Ehlmann, B., Fabre, C., Gasnault, O., Grotzinger, J., Lasue, J., Lewin, E., Leveille, R., McLennan, S., Maurice, S., Meslin, P.Y., Rapin, W., Rice, M., Squyres, S.W., Stack, K., Sumner, D.Y., Vaniman, D., Wellington, D., 2014. Calcium sulfate veins character-

ized by ChemCam/Curiosity at Gale crater, Mars. J. Geophys. Res., Planets 119, 1991–2016.
Poghosyan, A., Sturchio, N.C., Morrison, C.G., Beloso, A.D., Guan, Y.B., Eiler, J.M., Jackson, W.A., Hatzinger, P.B., 2014. Perchlorate in the Great Lakes: isotopic composition and origin. Environ. Sci. Technol. 48, 11146–11153.
Quinn, R.C., Martucci, H.F.H., Miller, S.R., Bryson, C.E., Grunthaner, F.J., Grunthaner, P.J., 2013. Perchlorate radiolysis on Mars and the origin of Martian soil reactivity. Astrobiology 13, 515–520.
Rao, B., Estrada, N., McGee, S., Mangold, J., Gu, B.H., Jackson, W.A., 2012a. Perchlorate production by photodecomposition of aqueous chlorine solutions. Environ. Sci. Technol. 46, 11635–11643.
Rao, B., Mohan, S., Neuber, A., Jackson, W.A., 2012b. Production of perchlorate by laboratory simulated lightning process. Water Air Soil Pollut. 223, 275–287.
Schauble, E.A., Rossman, G.R., Taylor, H.P., 2003. Theoretical estimates of equilibrium chlorine-isotope fractionations. Geochim. Cosmochim. Acta 67, 3267–3281.
Selverstone, J., Sharp, Z.D., 2015. Chlorine isotope behavior during prograde metamorphism of sedimentary rocks. Earth Planet. Sci. Lett. 417, 120–131.
Sharp, Z.D., Barnes, J.D., Brearley, A.J., Chaussidon, M., Fischer, T.P., Kamenetsky, V.S., 2007. Chlorine isotope homogeneity of the mantle, crust and carbonaceous chondrites. Nature 446, 1062–1065.
Sharp, Z.D., Mercer, J.A., Jones, R.H., Brearley, A.J., Selverstone, J., Bekker, A., Stachel, T., 2013. The chlorine isotope composition of chondrites and Earth. Geochim. Cosmochim. Acta 107, 189–204.
Sharp, Z.D., Shearer, C.K., Agee, C.B., McKeegan, K.D., 2011. The chlorine isotope composition of Mars. In: 42nd Lunar and Planetary Science Conference, p. 2534.
Sharp, Z.D., Shearer, C.K., McKeegan, K.D., Barnes, J.D., Wang, Y.Q., 2010. The chlorine isotope composition of the Moon and implications for an anhydrous mantle. Science 329, 1050–1053.
Shearer, C.K., Sharp, Z.D., McKeegan, K.D., Burger, P.V., McCubbin, F.M., 2014. Chlorine isotopic composition of martian meteorites. Implications for the composition of the martian crust and mantle, their interactions, and magmatic processes. In: 45th Lunar and Planetary Science Conference, p. 1502.
Smith, M.L., Claire, M.W., Catling, D.C., Zahnle, K.J., 2014. The formation of sulfate, nitrate and perchlorate salts in the martian atmosphere. Icarus 231, 51–64.
Stack, K.M., Grotzinger, J.P., Kah, L.C., Schmidt, M.E., Mangold, N., Edgett, K.S., Sumner, D.Y., Siebach, K.L., Nachon, M., Lee, R., Blaney, D.L., Deflores, L.P., Edgar, L.A., Fairen, A.G., Leshin, L.A., Maurice, S., Oehler, D.Z., Rice, M.S., Wiens, R.C., 2014. Diagenetic origin of nodules in the Sheepbed member, Yellowknife Bay formation, Gale crater, Mars. J. Geophys. Res., Planets 119, 1637–1664.
Sturchio, N.C., Bohlke, J.K., Beloso, A.D., Streger, S.H., Heraty, L.J., Hatzinger, P.B., 2007. Oxygen and chlorine isotopic fractionation during perchlorate biodegradation: laboratory results and implications for forensics and natural attenuation studies. Environ. Sci. Technol. 41, 2796–2802.
Sutter, B., Heil, E., Archer, P.D., Ming, D., Eigenbrode, J., Franz, H., Glavin, D., McAdam, A., Mahaffy, P., Niles, P.B., Stern, J.C., Navarro-Gonzalez, R., McKay, C., MSL Science Team, 2014. The investigation of magnesium perchlorate/iron phase mineral mixtures as a possible source of oxygen and chlorine detected by the Sample Analysis at Mars (SAM) instrument in Gale Crater, Mars. In: Eighth International Conference on Mars. Abstract 1140.
Sutter, B., Heil, E., Morris, R.V., Archer, P.D., Ming, D., Niles, P.B., Eigenbrode, J., Franz, H., Freissinet, C., Glavin, D., McAdam, A., Mahaffy, P., Martin-Torres, F.J., Navarro-Gonzalez, R., Paz-Zorzano, M., Stern, J.C., McKay, C., 2015. The investigation of perchlorate/iron phase mixtures as a possible source of oxygen detected by the Sample Analysis at Mars (SAM) instrument in Gale Crater, Mars. In: 46th Lunar and Planetary Science Conference, p. 2137.
Treiman, A., Bish, D., Ming, D., Grotzinger, J., Vaniman, D., Baker, M.B., Farmer, J., Chipera, S.J., Downs, R.T., Morris, R.V., Rampe, E., Blake, D., Berger, J., Cavanagh, P.D., Gellert, R., Glazner, A.F., Schmidt, M., Yen, A.S., Filiberto, J., 2015. Mineralogy and genesis of the Windjana sandstone, Kimberley area, Gale Crater, Mars. In: 46th Lunar and Planetary Science Conference, p. 2620.
Vaniman, D.T., Bish, D.L., Ming, D.W., Bristow, T.F., Morris, R.V., Blake, D.F., Chipera, S.J., Morrison, S.M., Treiman, A.H., Rampe, E.B., Rice, M., Achilles, C.N., Grotzinger, J.P., McLennan, S.M., Williams, J., Bell, J.F., Newsom, H.E., Downs, R.T., Maurice, S., Sarrazin, P., Yen, A.S., Morookian, J.M., Farmer, J.D., Stack, K., Milliken, R.E., Ehlmann, B.L., Sumner, D.Y., Berger, G., Crisp, J.A., Hurowitz, J.A., Anderson, R., Des Marais, D.J., Stolper, E.M., Edgett, K.S., Gupta, S., Spanovich, N., MSL Science Team, 2014. Mineralogy of a mudstone at Yellowknife Bay, Gale Crater, Mars. Science 343.
Wei, H.Z., Jiang, S.Y., Xiao, Y.K., Wang, J., Lu, H., Wu, B., Wu, H.P., Li, Q., Luo, C.G., 2012. Precise determination of the absolute isotopic abundance ratio and the atomic weight of chlorine in three international reference materials by the positive thermal ionization mass spectrometer-Cs_2Cl^+-graphite method. Anal. Chem. 84, 10350–10358.
Williams, J.T., Sharp, Z.D., Shearer, C.K., Agee, C.B., 2015. Confirmation of an isotopically light chlorine solar nebula and use of chlorine isotopes as a sensitive recorder of martian crustal contamination. In: 46th Lunar and Planetary Science Conference, p. 2641.